

Activities at J-PARC

H. Noumi^{1,2} for the J-PARC group

¹Research Center for Nuclear Physics (RCNP), Osaka University, Ibaraki, Osaka 567-0047, Japan

²Institute of Particle and Nuclear Studies (IPNS), KEK, Tsukuba, Ibaraki 305-0801, Japan

I. Charmed Baryon Spectroscopy at the J-PARC High-Momentum Beam Line

We are constructing a new platform of hadron physics under the MoU between RCNP, IPNS, and J-PARC at the J-PARC High-momentum Beam Line. We are preparing for an experiment on charmed baryon spectroscopy via the $p(\pi^-, D^{*-})$ reaction (E50) [1]. We report progress on some detector developments for E50 below.

A start counter, T0, is plastic scintillator hodoscopes, which will be used to define an incident pion and determine a time origin of the reaction. A plastic scintillator of $3\text{ mm} \times 3\text{ mm} \times 150\text{ mm}$ with an Multi-Pixel Photon Counter (MPPC) was tested at the Reserach Center for Electron Photon Science (ELPH) in Tohoku University, as illustrated in Fig. 1-left. The size of the scintillator slab is determined so as to keep a counting rate less than 3 MHz for a beam profile expected in the High-momentum Beam Line. A time resolution was as good as $70 \sim 75\text{ ps}$ for minimum-ionising particles ($\sim 600\text{ MeV}/c$ positrons). We expect that a Time of Flight (TOF) resolution will be able to achieve 100 ps or better between T0 and Resistive Plate Chambers [3]. We need a high-resolution Time to Digital Converter (HR-TDC) to digitize such high-speed signals. A proto-type of HR-TDC was developed. It demonstrated a time resolution as high as $\sim 20\text{ ps}$, as reported in this volume [2]. A fiber tracker is expected to be one of key detectors to measure particle trajectories in a high reaction rate

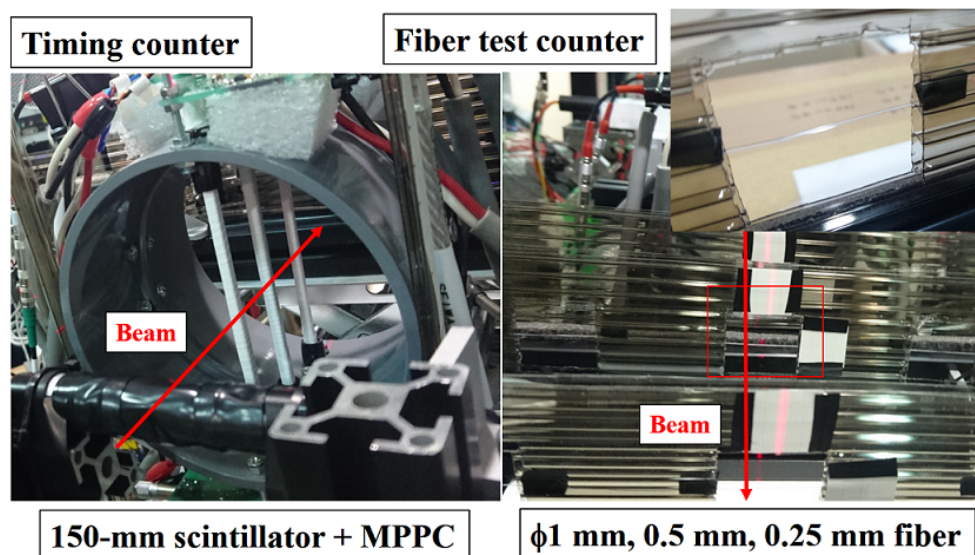


Figure 1: Setups of a beam test experiment for scintillator slabs (left) and scintillation fibers (right) at ELPH.

and high-particle multiplicity. Scintillating fibers with diameters of 1 mm, 0.5 mm, and 0.25 mm were tested at ELPH, as illustrated in Fig. 1-right. We detected 30, 14, and 6 of photo-electrons in average by MPPCs of $50\ \mu\text{m}$ pixel size for minimum-ionising particles ($\sim 600\text{ MeV}/c$ positrons) passing through the fibers of 1 mm, 0.5 mm, and 0.25 mm in diameter, respectively. In general, a smaller diameter fiber is advantageous to improve a momentum resolution of scattered particles. On the other hand, the 0.25-mm diameter fiber is expected to lose efficiency due to low photo-electron yields. We recognize that the 0.5-mm diameter fiber keeps a good efficiency with less materials. We will fabricate a proto-type of fiber tracker based on this test results.

There are several technical issues to construct the High-momentum Secondary Beam Line. At a view point of safety operation of high-power beam, designs of a production target, radiation shielding, and their maintenance scenario are of particular importance. For these designs, we are developing a simulation code based on MARS [4], which is commonly used to estimate radiation levels (including expected activations after beam irradiations) in high-energy particle accelerator facilities. This year, we have employed a specially appointed research fellow in charge of these design works under consultations of the Hadron Beam Line Group.

II. Study of Hyperon Resonances below $\bar{K}N$ threshold via the $d(K^-, n)$ reaction (E31)

The E31 experiment [5] aims at investigating the so-called double pole structure of $\Lambda(1405)$ [6] via the (K^-, n) reaction on a deuteron target. We carried out the first physics run in May and June, 2016 at the J-PARC K1.8BR beam line. About 30% of the approved beam time was allocated in 2016. As is already demonstrated in the pilot run done in 2015 [7], we immediately analyzed collected data. We successfully measured missing mass spectra of $d(K^-, n)X_{\pi^p m \Sigma^\mp}$, as shown in Fig. 2. The difference of the spectra was clearly observed, which occurs due to the interference term between the isospin $I = 1$ and $I = 0$ amplitudes in the final $\pi\Sigma$ state. We also measured a missing mass spectrum of $d(K^-, p)X_{\pi^-\Sigma^0}$, in which only the $I = 1$ state contributes. Comparing with the average of the $d(K^-, n)X_{\pi^p m \Sigma^\mp}$ spectra and the $d(K^-, p)X_{\pi^-\Sigma^0}$ spectrum, one sees that the strength of the latter spectrum is much smaller than that of the averaged spectrum. Assuming that the reaction mechanism of the $I = 1$ part in the $d(K^-, n)X_{\pi^p m \Sigma^\mp}$ reactions is similar to that of $d(K^-, p)X_{\pi^-\Sigma^0}$, we find that the $I = 0$ amplitude is dominant in the $d(K^-, n)X_{\pi^p m \Sigma^\mp}$ reactions. In the averaged spectrum, one can find structure below and above the K^-p threshold. A bump structure above the threshold is expected to be formed by a quasi-elastic scattering of \bar{K} followed by conversion processes $\bar{K}N \rightarrow \pi^\pm \Sigma^\mp$. The structure below the threshold carries information on a pole structure in the $\bar{K}N$ scattering.

We successfully identify Λ and missing $\pi^0\gamma$ in the $d(K^-, n)X_{\pi^0\Sigma^0}$ reaction, as shown in Fig. 4. We are sure to measure the $d(K^-, n)X_{\pi^0\Sigma^0}$ spectrum, which is a pure $I = 0$ channel in the final $\pi\Sigma$ state, in the 2nd run of E31 assigned in 2017. We will increase also the $d(K^-, n)X_{\pi^p m \Sigma^\mp}$ spectra by a factor of 3~4 in statistics in the 2nd run.

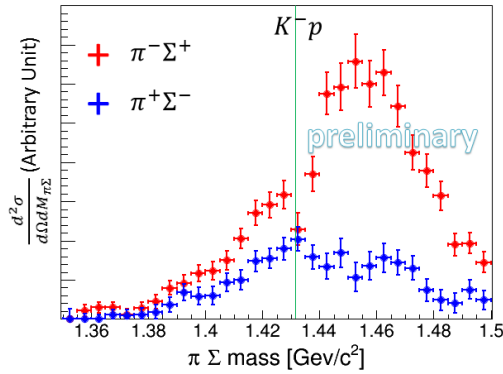


Figure 2: Missing mass spectra of $d(K^-, n)\pi^\pm\Sigma^\mp$

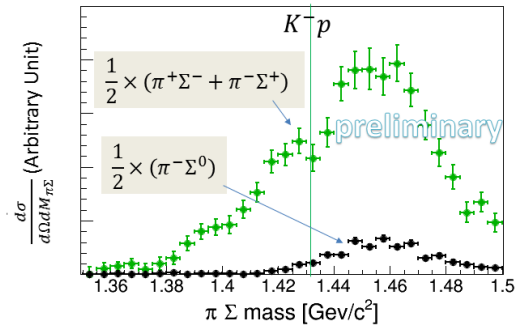


Figure 3: Averaged spectrum of $d(K^-, n)\pi^\pm\Sigma^\mp$ and a missing mass spectrum of $d(K^-, p)\pi^-\Sigma^0$ (divided by 2).

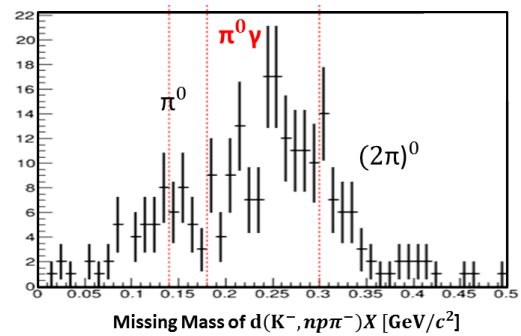
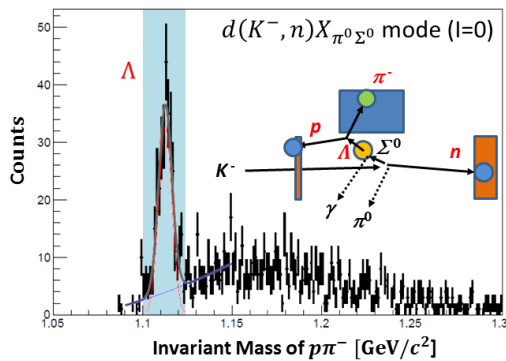


Figure 4: Invariant mass of a proton and a pion (left) and a missing mass spectrum of $d(K^-, n)\pi^0\gamma$ (right).

These works are partly supported by Grant-in-Aid for Scientific Research from JSPS [No. JP16H02188(A)].

References

- [1] J-PARC E50 proposal. http://www.j-parc.jp/researcher/Hadron/en/Proposal_e.html#1301
- [2] T.N. Takahashi *et al.*, “Development of a FPGA-based high resolution TDC using Xilinx Spartan-6”, this volume.

- [3] N. Tomida *et al.*, Nucl. Instrum. Meth. A766, 283(2014).
- [4] N.V. Mokhov, "The Mars Code System User's Guide", Fermilab-FN-628 (1995); O.E. Krivosheev, N.V. Mokhov, "MARS Code Status", Proc. Monte Carlo 2000 Conf., p. 943, Lisbon, October 23-26, 2000; Fermilab-Conf-00/181 (2000); N.V. Mokhov, "Status of MARS Code", Fermilab-Conf-03/053 (2003); N.V. Mokhov, K.K. Gudima, C.C. James et al, "Recent Enhancements to the MARS15 Code", Fermilab-Conf-04/053 (2004); <http://www-ap.fnal.gov/MARS/>.
- [5] J-PARC E31 proposal. http://www.j-parc.jp/researcher/Hadron/en/Proposal_e.html#0907
- [6] D. Jido, J. A. Oller, E. Oset, A. Ramos, and U.-G. Meissner, Nucl. Phys. A **725**, 181(2003).
- [7] H. Noumi for the J-PARC group, "Activities at J-PARC", RCNP annual report 2015.
- [8] S. Kawasaki *et al.*, Proc. of the 14th International Conference on Meson-Nucleon Physics and the Structure of the Nucleon (MENU2016), JPS Conf. Proc. 13, 020018(2017).